2018 European Control Conference (ECC)
June 12-15, 2018. Limassol, Cyprus

Generalized extended state observer design for the estimation of the rate of glucose appearance in artificial pancreas*

I. Sala, J.L. Díez and J. Bondia

Abstract— **Postprandial control is a relevant challenge in the context of glycemia regulation with an artificial pancreas for patients with type 1 diabetes. In general, pre-meal bolus schemes are adopted to cope with this problem. These schemes usually require individuals to announce the meal to the controller. As a result, control performance will be degraded if meal announcement is skipped or carbohydrates are misestimated by patients. An estimation of the rate of appearance could improve postprandial control without depending on meal announcement, since this variable could be employed either in meal detection algorithms, or in feedforward disturbance compensation techniques. This paper considers the viability of Generalized Extended State Observer in the estimation of the rate of appearance. A tuning procedure is presented to avoid overshoots in the estimation. Lastly, the observer is evaluated in an in-silico validation carried out by UVa-Padova simulator.**

I. Introduction

Type 1 diabetes is an autoimmune disorder in which the organism destroys pancreatic insulin-producing beta cells, which nullifies insulin secretion. Insulin is a hormone responsible of lowering plasma glucose concentration by promoting glucose regulation disposal by adipose tissue and muscle, and inhibiting hepatic glucose production. Consequently, plasma glucose levels remain too elevated (hyperglycemia) leading to severe microvascular complications [1]. For this reason, an exogenous insulin delivery is needed. Nevertheless, an excessive insulin infusion could be linked to hypoglycemia events, i.e., too low plasma glucose concentration, leading to coma or death [2] if they are not treated properly.

Artificial pancreas (AP) is a promising alternative to intensive insulin treatments. This is a closed-loop system that uses an insulin pump to deliver insulin according to interstitial glucose measurements coming from a continuous glucose monitoring sensor. Although several studies reported a tighter glucose control in AP compared to this fulfilled by open-loop control [3-5], meal compensation remains a challenge because of delays in insulin absorption and in glucose measurement [6]. In general, current AP systems cope with this challenge by delivering an insulin bolus at mealtime. Thus, patients must inform the controller about mealtimes and meal carbohydrate contents (CHO). However, patients not only tend to misestimate CHO but also to skip meal announcement, especially in adolescents, which implies a degradation of glucose control effectiveness [7].

Several meal detection algorithms have been proposed to manage unannounced meal compensation. Dassau et al. [8] suggested a voting scheme based on glucose derivative estimation to detect meals without estimating the meal start time or the meal size. A similar strategy, which includes CHO estimation computed by a finite impulse response filter, is proposed in [9]. Xie et al. [10] developed a variable state dimension algorithm where a switching function changes the state space model when a meal is detected to estimate meal size. Finally, Turskoy et al. [11] and Ramkissoon et al. [12] designed a meal detection and bolus calculation system based on a glucose rate of appearance estimation, that is, ingested carbohydrates effect on glucose increase.

Of note, the glucose rate of appearance could be regarded as an external disturbance in the insulin-glucose system, so then, a classical feedforward strategy could be used to mitigate its effect as an alternative to bolus delivery [13]. However, this disturbance is unknown, therefore, it must be estimated. The most of existing estimation techniques are based on complex multitracer oral glucose protocol or in glucose tolerant and meal tolerant tests [14], so they are limited to in-clinic studies and are difficult to be used for real-time control.

A significant amount of research has been focused in the development of disturbance estimation techniques, such as, disturbance observer [15], unknown input observer [16], equivalent input disturbance based estimation [17] or extended disturbance observer (ESO) [18]. The reader is referred to [19-21] and references therein for an exhaustive review. Among these techniques, ESO is highlighted because of its simplicity and its important role playing on Active Disturbance Rejection Control [22, 23]. Nonetheless, two factors constrain its application. On the one hand, ESO requires an integral chain system. On the other hand, it is only available when disturbances satisfy the so-called matching condition, i.e., disturbance enters at the same channel as the control input [21]. Despite being possible to apply a diffeomorphism to transform the system into an integral chain one [24], Li et al. [25] suggested a General Extended State observer (GESO) to deal with the limiting factors of ESO without any coordinate transformation.

This paper aims at the estimation of the rate of appearance through GESO design. The remaining of this paper is organized as follows. In Section II, both GESO and a reduced patient model for designing it, are introduced. Section III addresses the design procedure, highlighting the GESO gain tuning. In Section IV, GESO design is validated through

*This work was supported by the Spanish Ministry of Economy, Industry and Competitiveness (MINECO) through grants DPI2013-46982-C02-01-R and DPI2016-78831-C2-1-R, the European Union through FEDER funds and Generalitat Valenciana through grant ACIF/2017/021. I. Sala, J.L. Díez and J. Bondia are with the Instituto Universitario de Automática e Informática Industrial, Universitat Politècnica de València, Valencia, Spain. J.L. Díez and J. Bondia are also with the Centro de Investigación Biomédica en Red de Diabetes y Enfermedades Metabólicas Asociadas (CIBERDEM), Spain. (e-mails: ivsami@etsid.upv.es; jldiez@isa.upv.es; jbondia@isa.upv.es). Corresponding author: J. Bondia.

simulations in different scenarios. Finally, some conclusions are presented in Section V.

II. Background

A. Reduced Patient Model

Three main glucose-insulin models are available in AP for control purposes [26]: Bergman's minimal model [27], Identifiable Virtual Patient Model (IVP) [28] and Hovorka's model [29]. Among these, IVP model is a compromise option between accuracy and complexity, since it incorporates insulin absorption dynamics, which is not considered in Bergman's model, while it keeps a lower order than Hovorka's model. The IVP model equations are the following [28]:

$$\begin{cases} \dfrac{dI_{SC}(t)}{dt} = -\dfrac{1}{\tau_1} I_{SC}(t) + \dfrac{1}{\tau_1 CI} ID(t) \\ \dfrac{dI_p(t)}{dt} = -\dfrac{1}{\tau_2} I_p(t) + \dfrac{1}{\tau_2} I_{SC}(t) \\ \dfrac{dI_{EFF}(t)}{dt} = -p_2 I_{EFF}(t) + p_2 S_I I_p(t) \\ \dfrac{dG(t)}{dt} = -(GEZI + I_{EFF}(t))G(t) + EGP + R_A(t) \end{cases}, \quad (1)$$

where $I_{SC}(t)$ and $I_p(t)$ are subcutaneous and plasma insulin concentration (μU/mL), respectively; $I_{EFF}(t)$ is insulin effect to lower glucose (min^{-1}) and $G(t)$ is plasma glucose concentration (mg/dL). Additionally, $ID(t)$ is the exogenous subcutaneous insulin injection (μU/min) and $R_A(t)$ is the rate of glucose appearance (mg/dL/min). Finally, τ_1 and τ_2 are pharmacokinetic time constants (min), p_2 is the time constant for insulin action (min^{-1}), S_I is the insulin sensitivity (mL/ μU/min), *GEZI* is glucose effectiveness at zero insulin (min^{-1}), *EGP* is the hepatic glucose production (mg/dL/min) and *CI* is the insulin clearance (mL/min).

B. Generalized Extended State Observer

GESO is introduced in [25] for the single-input-single output non-integer chain system described in (2):

$$\begin{cases} dx(t)/dt = Ax(t) + b_u u(t) + b_d f(x, \omega(t), t) \\ y_m(t) = C_m x(t) \end{cases}, \quad (2)$$

where $x(t)$, $y_m(t)$ and $u(t)$ are the system state with dimension *n*, the measurable outputs (it may be different from output system) with dimension *r* and the control action input, respectively. $f(\cdot)$ is the lumped disturbance, that is, a signal that groups model uncertainties, possible time varying external disturbances $(\omega(t))$ and even nonlinear components of the system. Lastly, the system matrices are $A \in \Re^{nxn}, b_u \in \Re^{nx1}, b_d \in \Re^{nx1}$ and $C_m \in \Re^{rxn}$.

To estimate the lumped disturbance, state $x(t)$ is extended with $f(\cdot)$ giving rise to the following extended system:

$$\begin{cases} d\bar{x}(t)/dt = \bar{A}\bar{x}(t) + \bar{b}_u u(t) + E\,h(t) \\ y_m(t) = \bar{C}_m \bar{x}(t) \end{cases}, \quad (3)$$

where $\bar{x}(t) = \begin{bmatrix} x(t) & x_{n+1}(t) \end{bmatrix}^T = \begin{bmatrix} x(t) & f(\cdot) \end{bmatrix}^T$ is the extended state and $h(t) = \partial f(\cdot)/\partial t$ which is assumed to be 0, which means that lumped disturbance dynamics is slower than system dynamics. Matrices of the extended state system are defined in (4):

$$\bar{A} = \begin{bmatrix} A & b_d \\ 0_{1xn} & 0_{1x1} \end{bmatrix} \qquad \bar{b}_u = \begin{bmatrix} b_u \\ 0_{1x1} \end{bmatrix}$$
$$E = \begin{bmatrix} 0_{nx1} \\ 1_{1x1} \end{bmatrix} \qquad \bar{C}_m = \begin{bmatrix} C_m & 0_{rx1} \end{bmatrix} \quad . \quad (4)$$

Providing that $(\bar{A}, \bar{C}_m)$ satisfies the observability condition, then GESO is defined by the Luenberger-like observer

$$\begin{cases} d\hat{\bar{x}}(t)/dt = \bar{A}\hat{\bar{x}}(t) + \bar{b}_u u(t) + L(y_m(t) - \hat{y}_m(t)) \\ y_m(t) = \bar{C}_m \hat{\bar{x}}(t) \end{cases} . \quad (5)$$

In (5), $\hat{\bar{x}}(t) = [\hat{x}(t) \quad \hat{x}_{n+1}(t)]^T = [\hat{x}(t) \quad \hat{f}(\cdot)]^T$ are the estimates of system state and lumped disturbance; and $\hat{y}_m(t)$ is the estimate of the output. L is the observer gain that must be chosen so that $(\bar{A} - L\bar{C}_m)$ is Hurwitz for the system to be bounded-input bounded-output stable. As a result, if $f(\cdot)$ is bounded and $h(t)$ is null in stationary regime, then $\hat{\bar{x}}(t)$ will converge to $\bar{x}(t)$ asymptotically, as stated in [25]. These properties hold for the glucose rate of appearance.

III. Observer Design

A. General design procedure

A first approach to design the observer is including the nonlinear term $I_{EFF}(t)G(t)$ in the last equation of (1) into the lumped disturbance directly, that is,

$$f(\cdot) := R_A(t) - I_{EFF}(t)\,G(t) + EGP. \quad (6)$$

However, this uncouples the glucose system from the insulin system leading to a non-observable (A, C_m) pair, therefore, neither will the extended state system be observable, as pointed in [25]. With the goal of having an observable system while nonlinear term is kept in $f(\cdot)$ an approximation of the lumped disturbance $\tilde{f}(\cdot)$ is calculated by applying first-order Taylor series around the operating point $pf = [I_{SC}^0 \; I_p^0 \; I_{EFF}^0 \; G^0 \; R_A^0]$ resulting in,

$$\begin{aligned} \tilde{f}(\cdot) &= R_A(t) - R_A^0 - G^0(I_{EFF}(t) - I_{EFF}^0 - \\ &- I_{EFF}^0(G(t) - G^0) \end{aligned} . \quad (7)$$

Then, the last equation in (1) satisfies (8) around the operating point,

$$dG(t)/dt = -GEZI\,G(t) + f(t) + \tilde{f}(t) - \tilde{f}(t) \quad . \quad (8)$$

Thus, the patient model in (1) can be rewritten as (9), where $f'(\cdot)$ in (10) is the new lumped disturbance to be estimated by GESO:

$$\begin{cases} \dfrac{dI_{SC}(t)}{dt} = -\dfrac{1}{\tau_1} I_{SC}(t) + \dfrac{1}{\tau_1 CI} ID(t) \\ \dfrac{dI_p(t)}{dt} = -\dfrac{1}{\tau_2} I_p(t) + \dfrac{1}{\tau_2} I_{SC}(t) \\ \dfrac{dI_{EFF}(t)}{dt} = -p_2 I_{EFF}(t) + p_2 S_I I_p(t) \\ \dfrac{dG(t)}{dt} = -(GEZI + I^0_{IEFF}) G(t) - I_{EFF}(t) G^0 + f'(t) \end{cases}, \quad (9)$$

$$f'(t) = G^0 I_{EFF}(t) + I^0_{EFF}\, G(t) + f(t) \quad . \quad (10)$$

As a result, insulin system and glucose system are not uncoupled anymore. Then, defining $\bar{x} = [I_{SC}(t)\ \ I_p(t)\ \ I_{EFF}(t)\ \ G(t)\ \ f'(t)]^T$ and $y_m = G(t)$, the system matrices of the extended state system are obtained as:

$$\bar{A} = \begin{bmatrix} -1/\tau_1 & 0 & 0 & 0 & 0 \\ 1/\tau_2 & -1/\tau_2 & 0 & 0 & 0 \\ 0 & p_2 S_I & -p_2 & 0 & 0 \\ 0 & 0 & -G^0 & -(GEZI + I^0_{EFF}) & 1 \\ 0 & 0 & 0 & 0 & 0 \end{bmatrix} \quad \bar{b}_u = \begin{bmatrix} 1/\tau_1 CI \\ 0 \\ 0 \\ 0 \\ 0 \end{bmatrix} \quad . \quad (11)$$

$$E = [0\ \ 0\ \ 0\ \ 0\ \ 1]^T \qquad \bar{C}_m = [0\ \ 0\ \ 0\ \ 1\ \ 0]$$

It can be proved that $(\bar{A}, \bar{C}_m)$ satisfies the observability condition, so the observer in (5) can be designed. After that, an estimate of $R_A(t)$, $\hat{R}_A(t)$, can be calculated from (6) and (10) considering that $I_{EFF}(t) \cong \hat{\bar{x}}_3$, $G(t) \cong \hat{\bar{x}}_4$ and $f'(t) \cong \hat{\bar{x}}_5$.

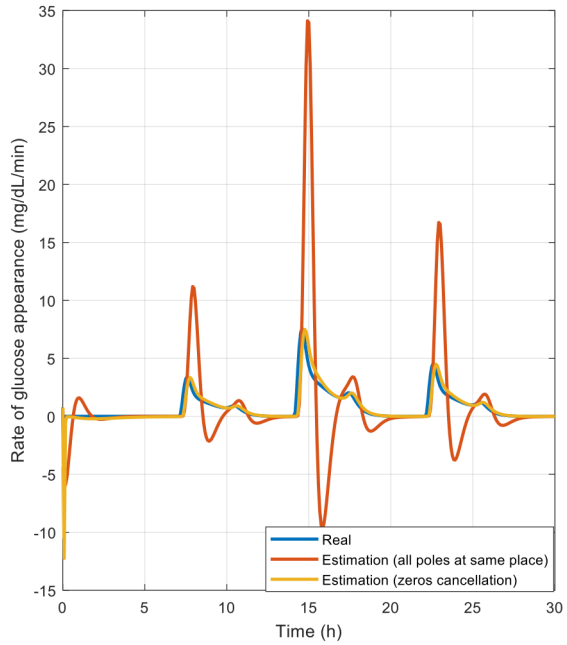

Figure 1. Comparison of the estimation of the rate of appearance when all poles are located at (s+w$_o$) and when zeros are cancelled.

B. Observer gain tuning

The next step is to define a gain L fulfilling that $(\bar{A} - L\bar{C}_m)$ is Hurwitz, as pointed in Section II.

A widespread approach for tuning GESO is to assign all the observer poles at $-\omega_0$, where ω_0 is the observer cut-off frequency, which is usually chosen as 3 or 5 times the closed-loop cut-off frequency [30]. A simulation in an ideal scenario is carried out to analyze this tuning. In this simulation, (1) is used as the plant model and the classical PD in (12) as the controller, where K_p is the proportional gain (U/min per mg/dL) and T_d (min) the derivative time, respectively; and G_{ref} is plasma glucose setpoint:

$$\begin{cases} u(t) = K_p\, e(t) + K_p\, T_d \dfrac{de(t)}{dt} \\ e(t) = y_{ref}(t) - y_m(t) = G_{ref}(t) - G(t) \end{cases} \quad . \quad (12)$$

As illustrated in red in Fig. 1 the overshoot degrades the estimation of the rate of appearance. Since no complex poles have been placed, it is necessary a further analysis to understand this behavior. The external representation of GESO in (5) is given by $\hat{\bar{x}}(t) = G(s)[u(s)\ \ y(s)]^T$ where s is the Laplace complex variable and $G(s)$ is the matrix of transfer functions defined as:

$$G(s) = \begin{bmatrix} g_{11}(s) & g_{12}(s) \\ g_{21}(s) & g_{22}(s) \\ g_{31}(s) & g_{32}(s) \\ g_{41}(s) & g_{42}(s) \\ g_{51}(s) & g_{52}(s) \end{bmatrix} . \quad (13)$$

From (13) it is straightforward to obtain,

$$\hat{f}'(s) = g_{51}(s) u(s) + g_{52}(s) y_m(s) . \quad (14)$$

Then, from the transfer functions derived from (9) and (12), (14) is rewritten as (15), where $h_{ref}(s)$ is a null transfer function when no model discrepancies exist and $h_f(s)$ is a transfer function defined by (16). Parameter l_5 in (16) is the last element in L.

$$\hat{f}'(s) = h_{ref}(s) y_{ref}(s) + h_f(s) f'(s) \quad (15)$$

$$h_f(s) = \frac{l_5 \left(s + \dfrac{1}{\tau_1}\right)\left(s + \dfrac{1}{\tau_2}\right)(s + p_2)}{(s + \omega_0)^{n+1}} \quad (16)$$

As shown above, the three zeros of $h_f(s)$ correspond to the open-loop poles of the insulin system. These zeros explain the overshoots. By placing three of the poles at $-1/\tau_1$, $-1/\tau_2$ and $-p_2$; and the remaining ones at $-\omega_0$, overdamped dynamics in the estimation is achieved, as depicted in yellow in Fig.1.

IV. In Silico Validation

In this section, UVa-Padova simulator [31] is employed to assess the behavior of the observer. This simulator, which is accepted by the Food and Drug Administration (FDA) for pre-clinical validations, is based on the Dalla Man's model [32]. It is a 13-state nonlinear system that allows a much more accurate simulation of glucose-insulin dynamics than IVP model does. To test control algorithms against realistic scenarios, several features where added to the simulator as meals of different CHO composition, changes of insulin sensitivity due to circadian rhythms and exercise. A cohort of virtual patients consisting of 10 adults, 10 adolescents and 10 children (plus an average subject in every group), is available in the educational version. In the following subsections evaluation metrics, scenarios and results are exposed.

A. Methodology

The parameters of the IVP model (1) are identified for the average adult patient in the UVa-Padova simulator, except insulin sensitivity, S_I, which is individualized for each patient in the cohort, giving rise to the parameter values shown in Table I.

TABLE I. IVP Parameters Used in Observer

Parameter	Value	Units
τ_1	82.82	min
τ_2	21.43	min
p_2	$1.549 \cdot 10^{-2}$	min^{-1}
S_I [a]	$6.923 \cdot 10^{-4}$ ($2.414 \cdot 10^{-4}$) $7.509 \cdot 10^{-4}$ [$4.435 \cdot 10^{-4}$]	mL/ μU/min
GEZI	$3.0300 \cdot 10^{-8}$	min^{-1}
EGP	1.4880	mg/dL/min
CI	1116.1250	mL/min

a. Insulin sensitivity is indicated as mean (standard deviation) and median [interquartile range] since it is the only parameter which has been individualized.

The GESO designed in Section III is discretized with a 5-min sample time by applying Tustin's transformation, since it preserves stability properties from the continuous model. Parameter ω_0 is chosen heuristically as a compromise between noise amplification and convergence velocity; and it is the same for the 10 virtual adults that are used in the simulation. Moreover, the operating point is calculated from (1) taking into account that G^0 is set equal to basal glucose and $R_A^0 = 0$ mg/dL/min. PD controller parameters are tuned as following: $Kp = -TDI/135000$ U/min per mg/dL (see [33] for further information) where TDI is the total daily insulin dose in U/day which is known from UVa-Padova simulator; and Td is set as 90 min. The goal of these simulations is to evaluate the estimation of the rate of appearance. At this stage, this estimation is not used for compensating meals through feedforward actions. Instead, a standard pre-meal bolus, as given by (17), is added to the PD output:

$$u_{bolus}(t) = g_{CHO} \cdot I2C \cdot \delta(t - t_{meal}) \tag{17}$$

where g_{CHO} (g) is the amount of CHO in the meal, $I2C$ (U/g) is the CHO-insulin ratio and $\delta(\cdot)$ is the Dirac delta and t_{meal} the beginning of the meal (min). Of note, pre-meal bolus is not as relevant in an observation problem as it is in a control one. However, other feedforward schemes triggered by meal detection algorithms or glucose rate of appearance estimation in fully automatic systems might lead to higher postprandial peaks, resulting in glucose moving away farther from the operating point. This might possibly imply degradation of the observer performance. This point requires further investigation.

In addition, two 30-h duration scenarios are simulated for the 10 adults of UVa-Padova simulator. In both of them, three meals of 45, 100 and 60 g CHO are consumed at 7, 14 and 22 h respectively. *Scenario 1* considers an ideal case, while *Scenario 2* simulates continuous glucose monitor sensor noise according to a 0.25-valued partial auto-correlation coefficient and model parameters variability, including:

- A meal-to-meal variability in intestinal absorption rate described by a uniform distribution of ±30% and CHO bioavailability following a uniform distribution of ±10% applied to the standard value of 0.9.
- Sinusoidal circadian S_I variation with 24-h period and random amplitude according to a uniform distribution of ±30% and random phase.

Finally, the quality of the estimation is evaluated with the area-under-the-curve (AUC) of the estimation of the rate of appearance and the root-mean-squared deviation (RMSD).

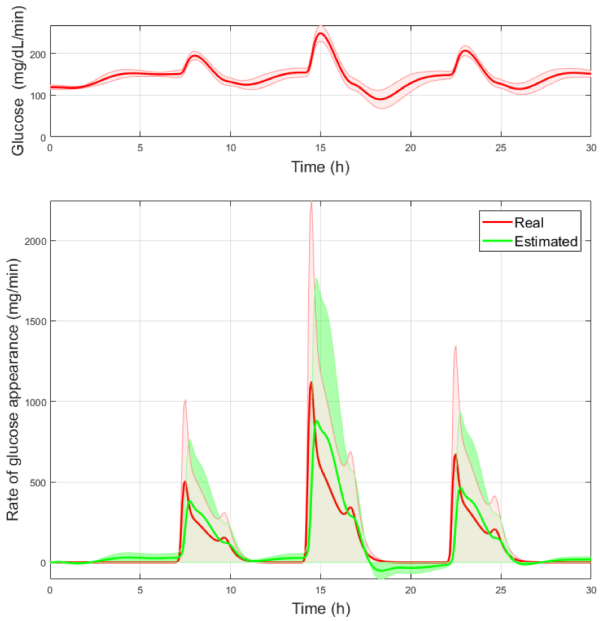

Figure 2. Plasma glucose (upper panel) and the rate of appearance value (bottom panel) for the 10 virtual adults in UVa-Padova simulator. Shaded areas correspond to standard deviation values while solid lines are mean values.

The real rate of appearance is computed from the UVa-Padova simulator and it is dependent on the subject, since each subject has its own meal model parameters in the simulator representing different absorption characteristics. Remark that the subject's meal model will be affected at each meal in *Scenario 2* by the variability introduced in the intestinal absorption rate and CHO bioavailability, as described above. To compute AUC, the estimates of rate of appearance are expressed in mg/min through the glucose distribution volume [30]. In this way, a perfect estimation for a given meal would imply an AUC value equal to the ingested amount of CHO times its corresponding bioavailability, considering enough time in the computation for its complete absorption.

B. Results

Fig. 2 depicts GESO estimations from the 10 virtual adult patients in *Scenario 1*. Compared to Fig.1, estimation is notably degraded due to model mismatch.

Mean RMSD values are 0.57 mg/dL/min for meal #1, 1.20 mg/dL/min for meal #2 and 0.67 mg/dL/min for meal #3. The largest error occurs for meal #2 as Table II shows. This is because the more glucose values increase, the farther it will be from designed operating point, since (7) will not be satisfied. In fact, the largest error in steady time takes place after the biggest meal (second meal) as illustrated in Fig.2. In [14] an off-line estimator of the rate of appearance offers, in a in silico validation, a RMSD=0.77 mg/dL/min for a 50-g meal. Additional clinical trials described in [14] achieved similar values (RMSD=0.61 mg/dL/min and RMSD=0.77 mg/dL/min) for a 78.5-g and 66.9-g absorbed CHO reference, respectively. However, those studies consider a more realistic scenario than the one used in this simulation.

In addition, mean AUC values are: 35.22 g, 88.63 g and 46.14 g for meal #1, meal #2 and meal #3, respectively, while the real ones should be 40.5 g, 90 g and 54 g, given that CHO bioavailability is 0.9 for all the cohort in the simulator. Despite model mismatch, differences in AUC are not significantly large, amounting to a 13%, 1.5% and 14.5% error respectively. Finally, the observer delay, i.e., time from real signal starts to increase to observer reaction, is less than 30 min in all patients.

About *Scenario 2*, as indicated in Table II, the addition of noise and variability increase RMSD values (0.645 mg/dL/min for meal#1, 1.653 mg/dL/min for meal #2 and 0.838 mg/dL/min for meal #3), although, they are still like RMSD values mentioned before. Mean AUC values of 40.42 g (meal #1), 75.74 g (meal #2) and 35.46 g (meal #3) may be acceptable considering that there is a random CHO bioavailability of ±10%.

TABLE II. OBSERVER PERFORMANCE METRICS FROM SIMULATIONS[a]

Meal	Scenario 1			Scenario 2		
	RMSD (mg/dL/min)	***AUC (g)***	***Observer delay (min)***	***RMSD (mg/dL/min)***	***AUC (g)***	***Observer delay (min)***
#1	0.567 (0.176)	35.22 (6.38)	29.0 (2.1)	0.645 (0.266)	40.42 (16.48)	25.0 (2.4)
#2	1.201 (0.374)	88.63 (12.94)	24.5 (1.6)	1.653 (0.714)	75.74 (42.70)	23.5 (2.4)
#3	0.682 (0.226)	46.14 (9.46)	28.0 (2.6)	0.838 (0.407)	35.46 (12.89)	27.5 (3.5)

a. Values are expressed as mean (standard deviation)

V. CONCLUSION

The relevance of an estimation of the glucose rate of appearance to improve postprandial control in the context of a fully automatic artificial pancreas is discussed, since this estimation can be used, not only as an input to meals detection algorithms, but also, it is possible to apply active disturbance rejection strategies with it.

Furthermore, a Generalized Extended State Observer, an alternative to Extended State Observer for non-integral chain systems, is designed to estimate the rate of appearance. Regarding the gain tuning procedure, placing all the poles at the same location has been shown that leads to an overdamping behavior, although these poles are real. This study concludes that the above behavior is due to zeros in the transfer function relating disturbance and its estimation, so cancelling these zeros significantly improves the estimation.

Finally, an in-silico evaluation reveals that the estimations are quite close to these that have been acquired by clinical procedures, even though the employed observer is simpler to design and to implement with respect to those techniques. However, observer convergence is slow, so, further research is needed to improve the estimation exactness. In this sense, a nonlinear tuning of the observer will be investigated. In addition, it will be studied a multiple operating point design to improve performance against large meals.

REFERENCES

[1] American Diabetes Association, "Diagnosis and Classification of Diabetes Mellitus", Diabetes Care, vol.1,pp. S62–S69, Jan.2010.

[2] P. E. Cryer, S. N. Davis y H. Shamoon, "Hypoglycemia in Diabetes", *Diabetes Care*,vol. 26, no. 6, pp.1902–1912, Jun. 2003.

[3] H.Thabit, A.Lubina-Solomon, M.Stadler et al, "Home use of closed-loop insulin delivery for overnight glucose control in adults with type 1 diabetes: a 4-week, multicentre, randomised crossover study", *Lancet Diabetes Endocrinol.*, vol.9, no.2, pp. 701–709, Sep. 2014.

[4] B.Kovatchev, P.Cheng, SM. Anderson et al, "Feasibility of Long-Term Closed-Loop Control: A Multicenter 6-Month Trial of 24/7 Automated Insulin Delivery", *Diabetes Technol Ther.*, vol. 1, no. 19, pp. 18–24, Jan. 2017.

[5] SK. Garg, SA. Weinzimer, WV. Tamborlane et al., "Glucose Outcomes with the In-Home Use of a Hybrid Closed-Loop Insulin Delivery System in Adolescents and Adults with Type 1 Diabetes", *Diabetes Technol. Ther.*, vol. 19, no. 3, pp. 155–163, Jan. 2017.

[6] A. Haidar, C. Duval, L. Legault, R. Rabasa-Lhoret, "Pharmacokinetics of insulin aspart and glucagon in type 1 diabetes during closed-loop operation", *J. Diabetes Sci. Technol.,* vol. 7, no. 6, pp. 1507–1512, Nov. 2013.

[7] A. S. Brazeau, H. Mircescu, K. Desjardins et al. , "Carbohydrate counting accuracy and blood glucose variability in adults with type 1 diabetes", *Diabetes Res. Clin. Pract.*, vol. 99, no. 1, pp. 19–23, Jan. 2013.

[8] E. Dassau, B.W. Bequette, B.A. Buckingham and F.J Doyle III, "Detection of a meal using continuous glucose monitoring: implications for an artificial beta-cell", *Diabetes Care*, vol. 2, no. 31, pp. 295–300, Feb. 2008.

[9] L. Hyunjin and B. W. Bequette, "A closed-loop artificial pancreas based on model predictive control: Human-friendly identification and automatic meal disturbance rejection", *Biomedical Signal Processing and Control*, vol.4, no. 4, pp. 347 – 354, Oct. 2009.

[10] J. Xie and Q. Wang, "Meal Detection and Meal Size Estimation for Type 1 Diabetes Treatment: A Variable State Dimension Approach", in *ASME 2015 Dynamic Systems and Control Conference*, Columbus, vol. 1, pp. V001T15A003 - V001T15A013, 2015.

[11] K. Turksoy, I. Hajizadeh, S. Samadi, et al., "Real-time insulin bolusing for unannounced meals with artificial pancreas", *Control Enginnering Practice,*vol. 59, pp. 159 – 164, Feb. 2017.

[12] C. H. Ramkisson, P. Herrero, J. Bondia and J. Vehí, "Meal Detection in the Artifcial Pancreas: Implications During Exercise", in *the 20th IFAC World Cong.*, *IFAC-PapersOnLine*, vol.50, no.1, pp. 5462 – 5467, Jul. 2017.

[13] G. Marchetti, B. Massimiliano, L. Jovanovic et al., "A Feedforward—Feedback Glucose Control Strategy for Type 1 Diabetes Mellitus", *J. Process Control*, vol. 18, no. 2, pp. 149–162, Feb. 2009.

[14] P. Herrero, J. Bondia, C. C. Palerm et al., "A Simple Robust Method for Estimating the Glucose Rate of Appearance from Mixed Meals", *J. Diabetes Sci. and Technol.,* vol. 6, no. 1, pp. 153 – 162, Jan. 2012.

[15] K. Ohishi, M. Nakao, K. Ohnishi, and K. Miyachi, "Microprocessor-Controlled dc motor for load-insensitive position servo system", *IEEE Trans. Ind. Electron*., vol. IE-34, no. 1, pp. 44–49, Feb. 1987

[16] C. Johnson, "Accommodation of external disturbances in linear regulator and servomechanism problems", *IEEE Trans. Autom. Control*, vol. AC-16, no. 6, pp. 635–644, Dec. 1971.

[17] JH. She, M. Mingxing, Y. Ohyama et al., "Improving Disturbance-Rejection Performance Based on an Equivalent-Input-Disturbance Approach", *IEEE Trans. Ind. Electron.*, vol. 55, no. 1, pp. 380–389, Jan. 2008.

[18] J. Han, "Extended state observer for a class of uncertain plants", *Control Decis.*, vol. 10, no. 1, pp. 85–88, 1995.

[19] W.-H. Chen, J. Yang, L. Guo y S. Li, "Disturbance-Observer-Based Control and Related Methods—An Overview", *IEEE Trans. Ind. Electron.*, vol. 63, no. 2, pp. 1083–1096, Feb. 2016.

[20] A. Radke and Z. Gao, "A Survey of State and Disturbance Observers for Practitioners", in *Proceedings of the 2006 American Control Conference*, Minneapolis, 2006.

[21] S. Li, J. Yang, W.-H. Chen and X. Chen, "Disturbance Observer-Based Control: Methods and Applications", Ed. CRC Press, 2014.

[22] J. Han, "From PID to active disturbance rejection control", *IEEE Trans.Ind. Electron*., vol. 56, no. 3, pp. 900–906, Mar. 2009.

[23] M. Baquero-Suárez, J. Cortes-Romero, J. Arcos-Legarda, H. Coral-Enriquez. "Automatic Stabilization of a Riderless Bicycle using the Active Disturbance Rejection Control Approach", *RIAI - Revista Iberoamericana de Automática e Informática Industrial*, vol. 15, no. 1, pp. 86–100, 2018.

[24] Z. Huang, X. Xiong, H. Wang et al., *Mathematical Problems in Engineering*, vol. 2016, pp. 1-9, Oct. 2016.

[25] S. Li, J. Yang, W.-H. Chen y X. Chen, "Generalized Extended State Observer Based Control for Systems With Mismatched Uncertainties", *IEEE Trans.Ind. Electron*, vol. 59, nº 12, pp. 4792 - 4802 , 2012.

[26] J.Bondia, S.Romero-Vivó, B.Ricarte y J. L. Díez, "Insulin Estimation and Prediction": A Review of the Estimation and Prediction of Subcutaneous Insulin Pharmacokinetics in Closed-Loop Glucose Control", *IEEE control systems*, vol.38, no.1, pp. 47 – 66. Feb. 2018.

[27] R. N. Bergman, L. S. Philips y C. Cobelli, "Physiologic Evaluation of Factors Controlling Glucose Tolerance in Man", *J. Clin. Invest*, vol. 68, pp. 1456-1467, 1981.

[28] S. Kanderian, S. A. Weinzimer y G. M. Steil, "The Identifiable Virtual Patient Model: Comparison of Simulation and Clinical Closed-Loop Study Results", *J. Diabetes Sci. Technol.*, vol. 6, nº 2, pp. 371-380, 2012.

[29] R. Hovorka, V. Canonico, L. J. Chassin et al, "Nonlinear model predictive control of glucose concentration in subjects with type 1 diabetes", *Physiological Measurement,* vol. 25, no. 4, pp. 905 – 920, Aug. 2004.

[30] Z. Gao, "Scaling and bandwidth-parameterization based controller tuning", in *Proceedings of the 2003 American Control Conference*, Denver, pp. 4989 – 4996, 2003.

[31] C. Dalla Man, F. Micheletto, D. Lv, M. Breton, B. Kovatchev y C. Cobelli, "The UVA/PADOVA Type 1 Diabetes Simulator: New Features", *J Diabetes Sci Technol*, vol. 8, no. 1, pp. 26-34, Jan. 2014

[32] C. Dalla Man, R. A. Rizza y C. Cobelli, "Meal Simulation Model of the Glucose-Insulin System", *IEEE Trans Biomed Eng.*,vol. 54, no. 10, pp. 1740 – 1749, Oct. 2007.

[33] C. C. Palerm, "Physiologic insulin delivery with insulin feedback: a control systems perspective", *Comput Methods Programs Biomed*., vol. 102, no. 2, pp. 130–137, May 2011.